Pure appl. geophys. 166 (2009) 131–152
0033–4553/09/010131–22
DOI 10.1007/s00024-004-0430-3

Pure and Applied Geophysics

Numerical Study of Tsunami Generated by Multiple Submarine Slope Failures in Resurrection Bay, Alaska, during the M_W 9.2 1964 Earthquake

ELENA SULEIMANI,[1] ROGER HANSEN,[1] and PETER J. HAEUSSLER[2]

Abstract—We use a viscous slide model of JIANG and LEBLOND (1994) coupled with nonlinear shallow water equations to study tsunami waves in Resurrection Bay, in south-central Alaska. The town of Seward, located at the head of Resurrection Bay, was hit hard by both tectonic and local landslide-generated tsunami waves during the M_W 9.2 1964 earthquake with an epicenter located about 150 km northeast of Seward. Recent studies have estimated the total volume of underwater slide material that moved in Resurrection Bay during the earthquake to be about 211 million m^3.

Resurrection Bay is a glacial fjord with large tidal ranges and sediments accumulating on steep underwater slopes at a high rate. Also, it is located in a seismically active region above the Aleutian megathrust. All these factors make the town vulnerable to locally generated waves produced by underwater slope failures. Therefore it is crucial to assess the tsunami hazard related to local landslide-generated tsunamis in Resurrection Bay in order to conduct comprehensive tsunami inundation mapping at Seward. We use numerical modeling to recreate the landslides and tsunami waves of the 1964 earthquake to test the hypothesis that the local tsunami in Resurrection Bay has been produced by a number of different slope failures. We find that numerical results are in good agreement with the observational data, and the model could be employed to evaluate landslide tsunami hazard in Alaska fjords for the purposes of tsunami hazard mitigation.

Key words: Landslide-generated tsunamis, numerical modeling, 1964 Alaska earthquake, Resurrection Bay, Seward.

1. Introduction

On March 28, 1964, the Prince William Sound area of Alaska was struck by the largest earthquake ever recorded in North America. This magnitude M_W9.2 megathrust earthquake generated the most destructive tsunami experienced in historical times by Alaskans and, further south, by people on the West Coast of the United States and Canada. Of the 131 fatalities associated with this earthquake, 122 were caused by tsunami waves (LANDER, 1996). Although tragic, the number of deaths was fortunately far smaller than in the case of the 2004 Indian Ocean tsunami due to low population density on the Alaska coast. As a result of the earthquake, more than twenty local tsunamis were

[1] Geophysical Institute, University of Alaska Fairbanks, 903 Koyukuk Dr., Fairbanks AK 99775-7320. E-mail: elena@gi.alaska.edu

[2] USGS, Alaska Science Center, 4210 University Dr., Anchorage, AK 99508-4626.

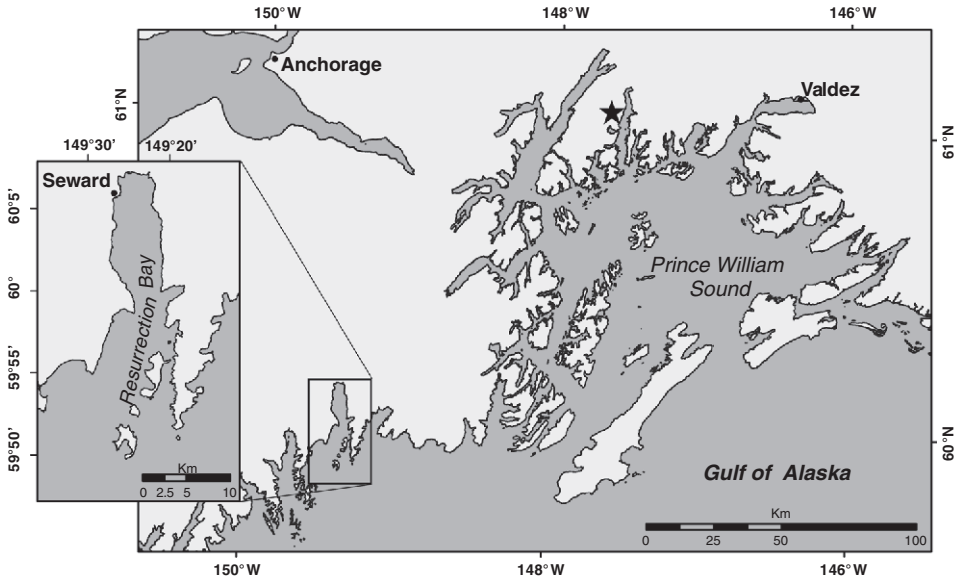

Figure 1
Location map of Resurrection Bay and Seward in the Gulf of Alaska. The star indicates the epicenter of the M_W 9.2 1964 earthquake.

generated by submarine and subaerial landslides in coastal Alaska, in addition to the major tectonic tsunami that was generated by displacement of the ocean bottom between the trench and the coastline. Local tsunamis caused most of the damage and accounted for 76% of the tsunami fatalities. Also, they arrived almost immediately after the shaking began, leaving no time for warning or evacuation. The community of Seward in Resurrection Bay (Fig. 1) suffered from the combined effects of local landslide-generated waves and the major tectonic tsunami that propagated from the main earthquake rupture zone in the Gulf of Alaska. The earthquake triggered a series of slope failures offshore of Seward, which resulted in landsliding of part of the coastline into the water, along with the loss of the port facilities. The town sustained great damage, and 12 people perished due to the tsunamis. Seward has grown considerably since the 1964 earthquake. As an ice-free harbor, it is an important supply center for Interior Alaska. The town is one of the major tourist destinations in Alaska. Seward hosts more than 90 cruise-ship dockings per year, and it is also a port for the state ferry system. Because local tsunamis were responsible for most of the damage and deaths in Seward during the 1964 earthquake, the future potential of similar events needs to be evaluated for comprehensive inundation mapping. Underwater slides could be triggered almost instantaneously during a future large earthquake, with tsunami waves arriving without warning, as they did in 1964. For tsunami hazard mitigation it is important to estimate the inundation areas, depths of inundation and velocity currents in Resurrection Bay.

Tsunamis caused by submarine slope failures are a serious hazard in glacial fjords of coastal Alaska and other high-latitude fjord coastlines. LEE *et al*. (2002) studied different environments of the US Exclusive Economic Zone and found that Alaskan fjords are likely the most susceptible environment to slope failures. In a fjord setting, rivers and streams drain the glacier that initially eroded the valley, forming a fjord-head delta and depositing sediment that easily looses strength during an earthquake. HAMPTON *et al*. (1996) note that in a fjord environment, where the deltaic sediment is deposited rapidly, the sediment builds up pore-water pressures and could liquefy under extreme low tide conditions or ground-shaking due to low static shear strength. BORNHOLD *et al*. (2001) identify the most common triggering mechanisms that can cause underwater slope failures as earthquakes, extreme low tides, and construction activities in ports and harbors. Because of these diverse mechanisms, prediction of landslide-generated tsunamis is a challenging task. Estimation of landslide tsunami risk for a coastal community requires assessment of locations of potential underwater failures using high-resolution bathymetry, known or reasonably estimated physical parameters of the underwater materials, and an adequate numerical model. The most probable locations of unstable sediment bodies in Resurrection Bay will be at the head of the bay where the Resurrection River had constructed a delta, and steep submarine slopes located elsewhere in the bay (HAEUSSLER *et al*., 2007).

This paper is the first numerical modeling study of tsunami waves in Resurrection Bay that utilizes the recent findings of the large-scale submarine slope failures in the bay during the 1964 earthquake (HAEUSSLER *et al*., 2007). It was shown that submarine failures initiated along the fjord walls at shallow depths and sediment was transported 6 to 13 km into the deepest part of the basin. The total volume of slide material that moved in Resurrection Bay during the earthquake was estimated to be about 211 million m^3 (HAEUSSLER *et al*., 2007). The purpose of this study is to recreate the sequence of tsunami waves observed in Resurrection Bay during the 1964 earthquake, and to test the hypothesis that the local tsunami was produced by a number of different slope failures. We perform numerical modeling of submarine slides and associated water waves and compare numerical results with the observations. In this preliminary analysis, our goal is not to model the inundation of dry land, but to create a foundation for future studies that will address runup of landslide-generated waves in Resurrection Bay. We will show that our modeling approach is a useful tool for estimating the landslide tsunami hazard at Seward and other tsunami-prone communities in southern Alaska.

2. Tsunami Hazard in Resurrection Bay

Resurrection Bay is a deep glacial fjord, typical of many in south-central and southeastern Alaska. KULIKOV *et al*. (1998) analyzed tsunami catalog data for the North Pacific Coast and showed that this region has a long history of tsunami waves generated by submarine and subaerial landslides, avalanches and rockfalls. The authors also found

Figure 2 ▶

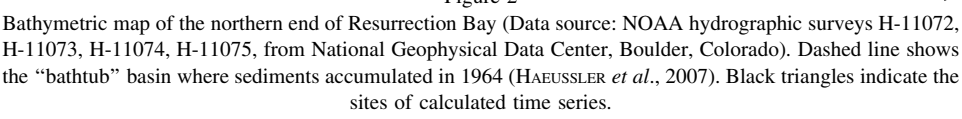

Bathymetric map of the northern end of Resurrection Bay (Data source: NOAA hydrographic surveys H-11072, H-11073, H-11074, H-11075, from National Geophysical Data Center, Boulder, Colorado). Dashed line shows the "bathtub" basin where sediments accumulated in 1964 (HAEUSSLER *et al*., 2007). Black triangles indicate the sites of calculated time series.

that, in the majority of cases, tectonic tsunamis that arrive in bays and fjords from the open ocean have relatively small amplitudes, but a great number of local landslide-generated tsunamis have considerably larger wave amplitudes. For example, as a result of the 1964 earthquake, about 20 local submarine and subaerial landslide tsunamis were generated in Alaska (LANDER, 1996). Following the earthquake, Seward was the only place hit by both landslide-generated tsunamis and a major tectonic tsunami (HAEUSSLER *et al*., 2007), while several other communities experienced only locally generated waves (PLAFKER *et al*., 1969). KULIKOV *et al*. (1998) also noted that, due to the sparse population of the area, the actual number of historical landslide tsunami events is unknown, and probably much greater than the number of events observed or recorded. BORNHOLD *et al*. (2001) addressed the problem of estimation of risk from landslide-generated tsunami waves for the coast of Alaska and British Columbia. They outlined the specific features of the long-term prediction of landslide-generated tsunamis at selected sites, and developed an approach for estimating tsunami risk. The long-term approach consists of two steps: analysis of historical events and verification of model results with runup observations at the site; and numerical simulation of hypothetical tsunami scenarios. Although for many communities historical observations do not exist, Seward is an exception. The effects of the 1964 earthquake and tsunami waves in Resurrection Bay, including wave amplitudes and extent of inundation, are well documented (WILSON and TØRUM, 1968; LEMKE, 1967) and are ideal for numerical modeling studies.

2.1. Study Area and Tsunami Waves of March 28, 1964

The town of Seward is located at the northwest corner of Resurrection Bay, and is built mostly on the alluvial fan of Lowell Creek. Lowell Point, Tonsina Point, and the Fourth of July Creek (Fig. 2) are locations of other alluvial fans that extend into the bay as fan deltas (LEMKE, 1967). The entire head of Resurrection Bay is a fjord-head delta that was built by the Resurrection River. HAEUSSLER *et al*. (2007) used the word "bathtub" to describe a flat depression in the middle of the bay extending north to south (Fig. 2). The deepest part of the bathtub is about 300 meters. The average pre-earthquake offshore slopes in the vicinity of Seward ranged from 10° to 20°, decreasing to 5° at the depth of about 200 m (LEMKE, 1967). Today, the same area has an average slope of about 25° (LEE *et al*., 2006). A natural barrier formed by Caines Head and a glacial sill divide the bay into two deep basins, separated by a narrow "neck" with maximum depth above the sill of 195 m. This sill inhibits sediment transport by tidal currents to the southern part of the bay (HAEUSSLER *et al*., 2007). Our study focuses on the northern basin of Resurrection Bay, north of the sill area (Fig. 2).

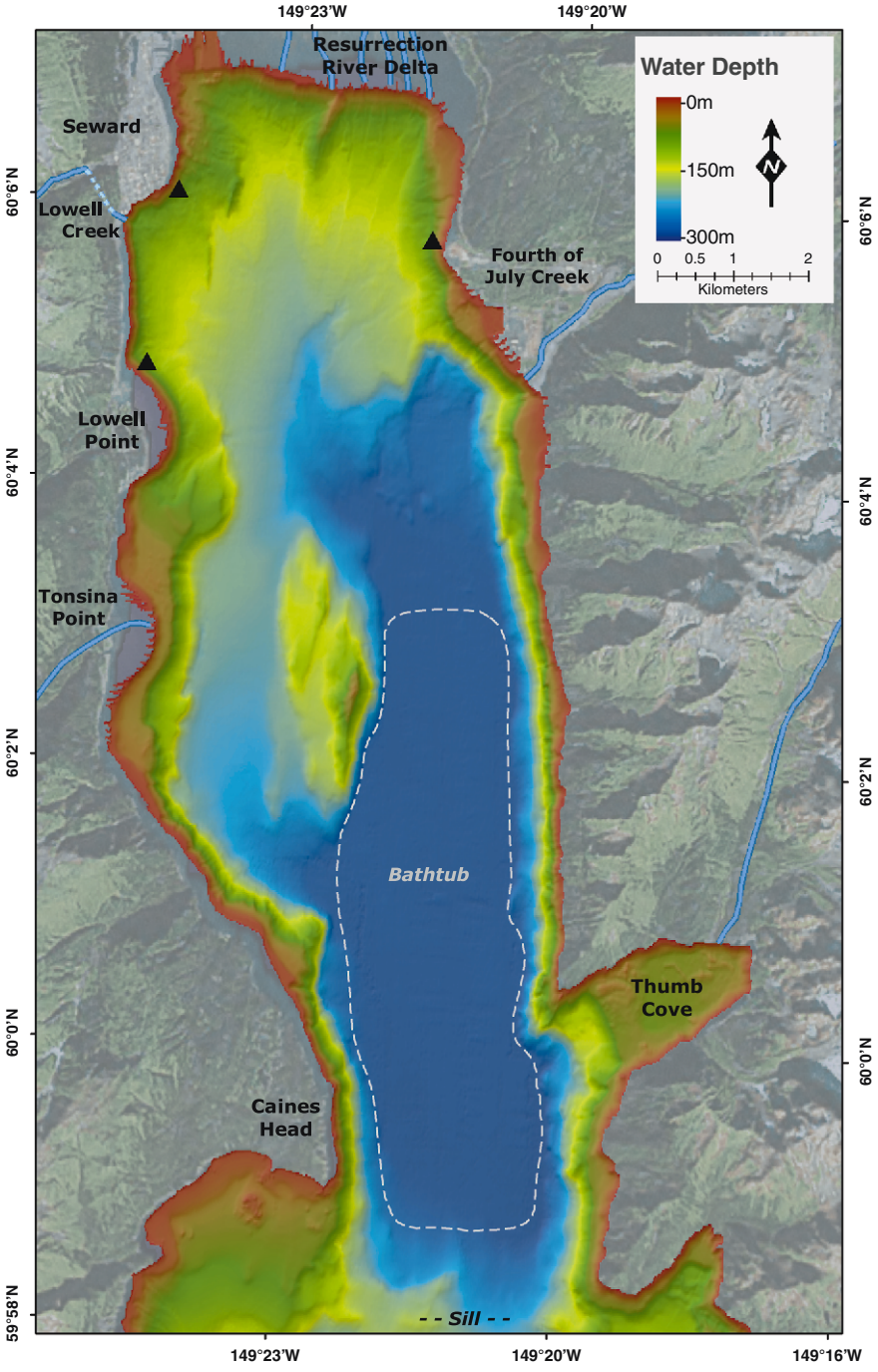
149°23'W
149°20'W
Resurrection River Delta
Seward
Lowell Creek
Fourth of July Creek
Lowell Point
Tonsina Point
Bathtub
Thumb Cove
Caines Head
- - Sill - -
Water Depth
0m
150m
300m
0 0.5 1 2
Kilometers
N
60°6'N
60°4'N
60°2'N
60°0'N
59°58'N
149°16'W

There were several types of waves observed in Resurrection Bay on March 28, 1964: landslide-generated waves, a tectonic tsunami wave train, and probably seiches (WILSON and TØRUM, 1968), all resulting in a complicated wave pattern. The Seward tide gauge was located on a dock that collapsed into the bay as a result of massive submarine slope failures. The instrument was heavily damaged, and the record was lost. Although the sequence of waves was reconstructed from observations provided by eyewitnesses, there are uncertainties in the time estimates of wave arrivals (WILSON and TØRUM, 1968). Table 1 is a portion of the eyewitness report compiled by WILSON and TØRUM (1968) that covers the period when the ground was shaking. An initial drawdown of water was observed at the Seward waterfront about 30 seconds after the ground started to shake. At the same time, fuel tanks ruptured, leaked, and subsequently exploded; the tanks slid into the bay, and the receding water was covered with burning oil. The highest wave at Seward was about 6–8 m high observed about 1.5-2 minutes after the shaking began (Table 1). The tectonic tsunami wave, covered with burning oil, came into the bay about 25 minutes after the earthquake, spanning the entire width of the bay (WILSON and TØRUM, 1968). This wave was as high as the initial landslide-generated waves. Because the source of local waves in the bay ceased at the end of ground-shaking (WILSON and TØRUM, 1968), about 20 minutes before the arrival of the tectonic tsunami, we can assume that these events are independent, and model them separately. In this paper we focus only on waves generated by local submarine slope failures in Resurrection Bay.

2.2. *Justification for the Study*

Geologic investigations were conducted in the Resurrection Bay area right after the earthquake by several researchers (LEMKE, 1967; WILSON and TØRUM, 1968; PLAFKER *et al.*, 1969; SHANNON and HILTS, 1973). From these studies, it was concluded that strong ground motion during the earthquake caused several submarine slope failures along the Seward waterfront and other areas within upper Resurrection Bay. HAMPTON et al. (1996) described the triggering mechanism as dynamic forces imposed by large seismic accelerations that added to the downslope component of the gravitational force on the

Table 1

Observations at Seward waterfront during the earthquake (from WILSON and TØRUM, 1968)

Estimated time points and heights (zero time is at the start of the quake)			
Whiteness	Source	Time	Feet
Ted Pedersen		30 seconds	Drawdown at Standard Oil Dock
Hal Gilfillen	Genie Chance	45 ”	
Robert Clark		45 ”	
Many Eyewitnesses	Genie Chance	1.5–2 minutes	+20–25 feet at ARR docks
	BERG *et al.* (1964)		Rose over box cars on RR tracks
	LANTZ and KIRKPATRICK (1964)		Reached corner of Third Avenue and Washington

steep slopes of the Lowell Creek and Resurrection River deltas. HAMPTON *et al*. (2002) notes that the stability of the sediment was also decreased by the low tidal level at the time of the earthquake, and by the rapid drawdown of water due to the initial slope failure, which prevented the pore water from draining from the sediment quickly enough to maintain hydrostatic conditions. The underwater slope failures generated large waves that were observed during ground shaking (WILSON and TØRUM, 1968). The major factors that contributed to the total volume and aerial extent of the slide material were the long duration of ground motion (3 to 4 min), the configuration of underwater slopes, and the type of sediment forming these slopes, unconsolidated and fine-grained materials (LEMKE, 1967). HAMPTON *et al*. (1996) added that high artesian pressure within aquifers of the delta combined with the extra load caused by waterfront artificial fill and the shoreline development also contributed to the slope failures. The authors summarized all the environmental loads in Resurrection Bay and concluded that although it was a unique combination of conditions, most of them had been documented separately during slope failures in other fjords.

Studies by LEE *et al*. (2006) and HAEUSSLER *et al*. (2007) provided analysis of pre- and post-earthquake bathymetric data and high resolution subbottom profiles of Resurrection Bay and showed convincing evidence of massive submarine landsliding. They utilized a 2001 NOAA high-resolution multibeam bathymetry survey of Resurrection Bay to study the morphology and depth changes of the fjord bottom. A shaded relief map derived from this bathymetric data shows a variety of sea-floor features related to submarine slides. LEE *et al*. (2006) identified remains of the Seward waterfront that failed in 1964 as a result of strong ground-shaking. These remains are visible as blocky debris extending offshore Seward for about 750 m (Fig. 3). The authors also identified dispersed debris flows that correspond to failures of the Resurrection River delta, and they concluded that the 1964 earthquake could potentially have triggered different failure types simultaneously. HAEUSSLER *et al*. (2007) concluded that several failures initiated along the fjord walls at relatively shallow depths, and the mass flows produced by these failures transported most of the material as far as 6 to 13 km into the bathtub, covering the entire basin with a flow deposit.

Engineering studies conducted after the 1964 earthquake (LEMKE, 1967) showed that additional onshore and submarine landslides can be expected along the Seward waterfront in the event of another large earthquake, and that sediment from the Resurrection River and smaller creeks will continue to accumulate on underwater slopes of Resurrection Bay. The recent results of sediment chemistry monitoring in Port Valdez, located in a glacial fjord setting similar to that of Resurrection Bay (Fig. 1), demonstrated high sediment accumulation rates of about 1.5 cm/year at the head of the fjord (SAVOIE *et al*., 2006). Sediment could be released not only by the ground-shaking due to an earthquake, but also by other triggering events, such as extreme low tide conditions and construction activities. Because short-term prediction of landslide tsunamis is not applicable for tsunami risk assessment (BORNHOLD *et al*., 2001), we will need to use the long-term approach described at the beginning of section 2 for estimating the local

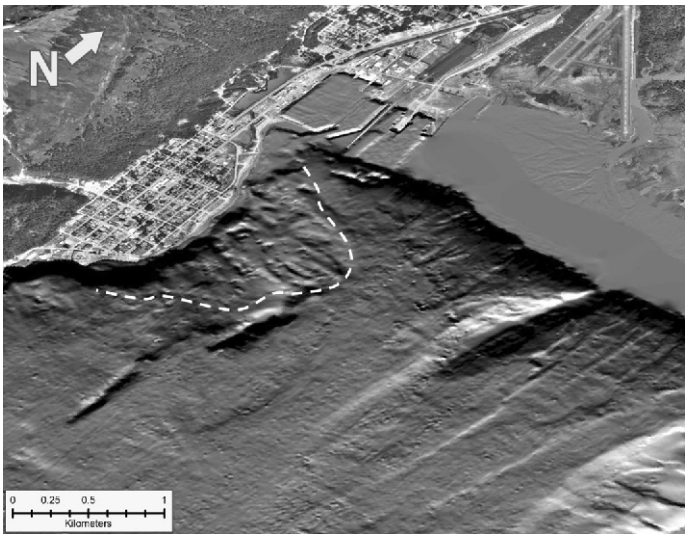

Figure 3
Oblique bathymetric image, overlain with aerial photograph, of the northwest corner of Resurrection Bay, offshore of the Seward waterfront. Dashed line delineates the blocky debris that are remains of the 1964 waterfront failure. The scale was made for the downtown Seward.

tsunami hazard at Seward. The essential part of this approach is numerical modeling of historical landslide tsunami events, as well as simulating future hypothetical underwater slope failures.

3. Model Description

A number of studies of tsunami waves generated by landslides employed depth-integrated numerical models. HARBITZ (1992) simulated tsunamis generated by Storegga slides using linear shallow water equations. JIANG and LEBLOND (1992, 1994), FINE *et al.* (1998), THOMSON *et al.* (2001), IMAMURA *et al.* (2001), TITOV and GONZALEZ (2001) used nonlinear shallow water approximation to model the slide-water system as a two-layer flow. LYNETT and LIU (2002) discussed the limitations of the depth-integrated models with regards to landslide-generated waves, and developed fully nonlinear weakly dispersive model for submarine slides that is capable of simulating waves from relatively deep water to shallow water. The model was later extended to employ the multilayer approach (LYNETT and LIU, 2004a, 2004b) that allowed for accurate simulation of landslides in shallow and intermediate water (LYNETT and LIU, 2005). GRILLI and WATTS (2005) derived and validated a two-dimensional fully nonlinear dispersive model that does not have any restrictions on tsunami amplitude, wavelength, or landslide depth, and describes the motion of the landslide by that of its center of mass.

To simulate tsunami waves produced by multiple underwater slope failures in Resurrection Bay on March 27, 1964, we use a three-dimensional numerical model of a viscous underwater slide with full interactions between the deforming slide and the water waves that it generates. This model was initially proposed by JIANG and LEBLOND (1994). FINE *et al*. (1998) improved the model by including realistic bathymetry, and also by correcting errors in the governing equations. The model assumptions as well as its applicability to simulate underwater mudflows are discussed by Jiang and LeBlond in their formulation of the viscous slide model (JIANG and LEBLOND, 1992, 1994). The model uses long-wave approximation for water waves and the deforming slide, which means that the wavelength is considerably greater than the local water depth, and the slide thickness is considerably smaller than the characteristic length of the slide along the slope (JIANG and LEBLOND, 1994). ASSIER-RZADKIEWICZ *et al*. (1997) argued that the long-wave approximation could be inaccurate for steep slopes, that is for slopes greater than 10°. RABINOVICH *et al*. (2003) studied the validity of the long-wave approximation for slopes greater than 10° and found that for the slope of 16° the possible error was 8%, and for the maximum slope in their study of 23° the possible error was 15%. Based on this analysis, for the average pre-earthquake offshore slopes that ranged from 10° to 20° in the vicinity of Seward, the possible error introduced by a slide moving down these higher gradient slopes could be around 10%.

The advantage of the vertically integrated model that includes two horizontal dimension effects is its ability to simulate real landslide tsunami events using high-resolution numerical grids based on multibeam bathymetry data. Although model runs require use of high-performance computing, the computational times are still reasonable. This model was successfully applied to simulate tsunami waves in Skagway Harbor, Alaska, generated by collapse of the PARN dock on November 3, 1994 (FINE *et al*., 1998; THOMSON *et al*., 2001). The results of numerical simulations were in good agreement with the tide gauge record in Skagway Harbor, one of the numerous fjords in southeastern Alaska. RABINOVICH *et al*. (2003) simulated potential underwater landslides in British Columbia fjords, settings that are similar to Resurrection Bay, and demonstrated that this model can be used for tsunami hazard assessment.

3.1. Model Equations

The geometry of the slide is shown in Figure 4. The physical system consists of two layers: The upper one is water with density ρ_1, and the lower layer is slide material with density ρ_2 and dynamic viscosity μ. The slide is assumed to be an incompressible viscous fluid. We assume a sharp interface between the layers, with no mixing allowed between water and sediments. The disturbance of the water surface produced by slide motion is described by free surface elevation $\xi(x, y, t)$ and horizontal components of water velocity $u(x, y, t)$ and $v(x, y, t)$. The horizontal velocity of the slide $\mathbf{U}$ has components $U(x, y, t)$ and $V(x, y, t)$. The thickness of the slide is $D(x, y, t)$, the undisturbed water depth is $H(x, y)$, and $H_t(x, y, t) = H + \xi - D$ is the total water depth above the slide. The equations for the

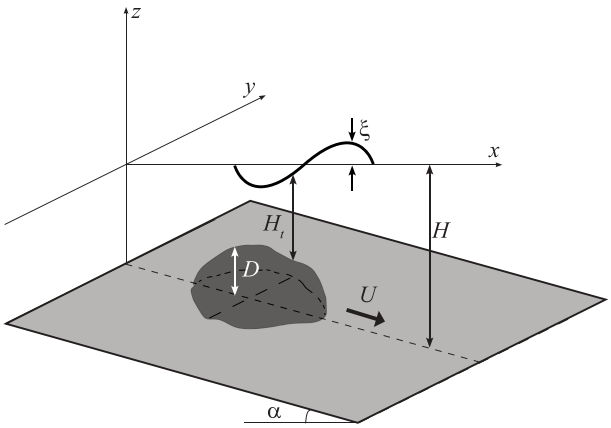

Figure 4
Geometry of a submarine landslide.

slide were initially derived under the assumption that the underwater slide rapidly reaches its equilibrium velocity (JIANG and LEBLOND, 1994), which means that changes of horizontal components of the slide velocity in the vertical direction can be approximated by a parabolic function. It is also assumed that the slide mass does not cross the boundary of the computational domain.

The slide equations that we use in this study are the equations from JIANG and LEBLOND (1994) that were corrected by FINE *et al*. (1998):

$$\frac{\partial U}{\partial t} - \frac{1U}{5D}\frac{\partial D}{\partial t} + \frac{4}{5}\left(U\frac{\partial U}{\partial x} + V\frac{\partial U}{\partial y}\right) = -\frac{3}{2}g\left(\frac{\partial D}{\partial x} - \frac{\partial H}{\partial x}\right) - \frac{3}{2}g\frac{\rho_1}{\rho_2}\frac{\partial H_t}{\partial x} - \frac{3\mu U}{\rho_2 D^2}, \quad (1)$$

$$\frac{\partial V}{\partial t} - \frac{1V}{5D}\frac{\partial D}{\partial t} + \frac{4}{5}\left(U\frac{\partial V}{\partial x} + V\frac{\partial V}{\partial y}\right) = -\frac{3}{2}g\left(\frac{\partial D}{\partial y} - \frac{\partial H}{\partial y}\right) - \frac{3}{2}g\frac{\rho_1}{\rho_2}\frac{\partial H_t}{\partial y} - \frac{3\mu V}{\rho_2 D^2}, \quad (2)$$

$$\frac{\partial D}{\partial t} = -\frac{2}{3}\left(\frac{\partial (DU)}{\partial x} + \frac{\partial (DV)}{\partial y}\right). \quad (3)$$

The equations that describe the upper layer are the nonlinear shallow water equations:

$$\frac{\partial u}{\partial t} + u\frac{\partial u}{\partial x} + v\frac{\partial u}{\partial y} = -g\frac{\partial \xi}{\partial x}, \quad (4)$$

$$\frac{\partial v}{\partial t} + u\frac{\partial v}{\partial x} + v\frac{\partial v}{\partial y} = -g\frac{\partial \xi}{\partial y}, \quad (5)$$

$$\frac{\partial H_t}{\partial t} = -\frac{\partial (H_t u)}{\partial x} - \frac{\partial (H_t v)}{\partial y}. \quad (6)$$

The variable that couples the two systems of equations is the total water depth above the slide, $H_t(x, y, t)$. In this study we do not calculate the inundation of dry land due to

landslide-generated waves, which implies that the normal velocity component is set to zero at the shoreline. At the open boundary, we apply the radiation boundary condition for surface waves.

3.2. Data

The two data sets used in this study are the bathymetry of Resurrection Bay, and the initial distribution and thickness of the slide material. In order to simulate underwater slope failures of 1964 in Resurrection Bay, we use a bathymetry grid of 15-m resolution that covers the northern part of the bay (Fig. 2). The source of the data is the 2001 NOAA high-resolution multibeam survey of Resurrection Bay, and the 2006 survey of the Seward harbor and surrounding areas (LABAY and HAEUSSLER, 2008, in press).

HAEUSSLER *et al*. (2007) have conducted a comprehensive study of submarine slope failures in Resurrection Bay during the 1964 earthquake. The location and extent of submarine mass failures were estimated based on analysis of pre- and post-earthquake bathymetry. The authors created a bathymetric difference grid that shows depth changes in the bay resulting from the 1964 slope failures. The estimated total volume of slide material is 211 million m^3 (HAEUSSLER *et al*., 2007). A map of the slide thickness, derived from the bathymetric difference grid, is shown in Figure 5. This distribution of the slide material serves as an initial condition for the slide surface in system of equations (1)–(3). HAEUSSLER *et al*. (2007) identified ten different landslide areas and calculated their volumes (Fig. 5). We use their results shown in Figure 5 to better understand the contribution of different slide complexes to the observed tsunami amplitudes in Resurrection Bay.

4. Numerical Simulation of the 1964 Landslides and Tsunami

We use an explicit in time finite-difference method to numerically solve equations (1)–(6) on a staggered leap-frog grid. Thomson *et al*. (2001) describe the construction of the numerical scheme and provide the final discretized equations. The computational domain is shown in Figure 2. This area is covered by a grid of 711 $\times$ 1310 grid points with horizontal space steps $\Delta x = 13.75$ m and $\Delta y = 15$ m, and time step $\Delta t = 0.01$ sec. SHANNON and HILTS (1973) conducted a subsurface geotechnical investigation of materials that failed in Resurrection Bay during the 1964 earthquake. They found that the density of the slide material ranged from 2.0 $g \cdot cm^{-3}$ to 2.11 $g \cdot cm^{-3}$. We do not have any measurements of the slide viscosity, but sensitivity studies by RABINOVICH *et al*. (2003) demonstrated that the influence of kinematic viscosity on tsunami wave heights is small. We assume slide density of $\rho = 2.0$ $g \cdot cm^{-3}$ and slide viscosity of $\mu = 0.05$ $m^2 \cdot s^{-1}$. The upper and lower surfaces of the slide mass are defined by the initial slide thickness distribution (Fig. 5), and they are given on the same 711 $\times$ 1310 grid used for bathymetric data. The slide thicknesses are added to the bathymetry values in order to

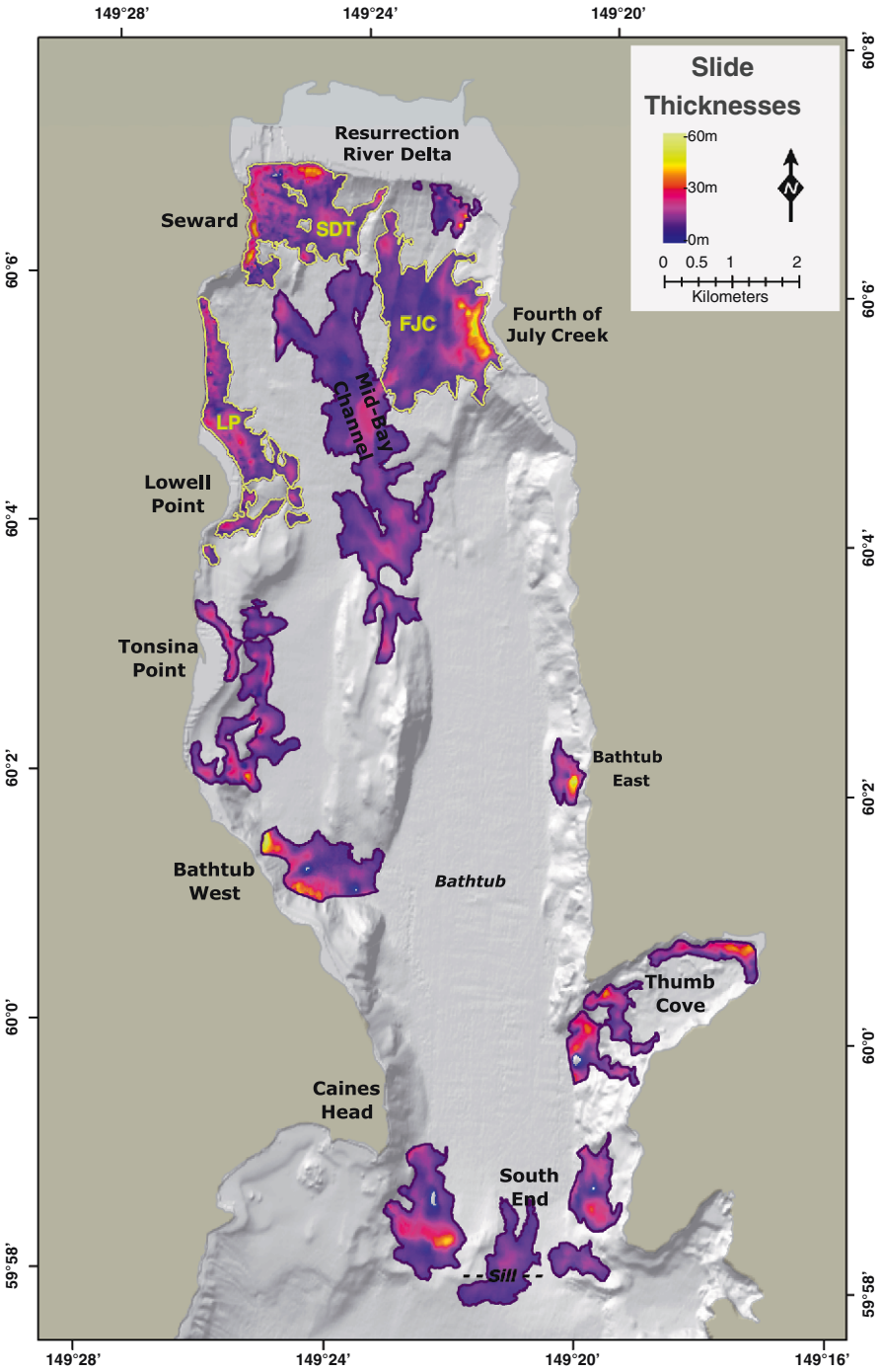
149°28'
149°24'
149°20'
149°16'
60°8'
60°6'
60°4'
60°2'
60°0'
59°58'
Slide
Thicknesses
60m
30m
0m
0 0.5 1 2
Kilometers
N
Resurrection
River Delta
Seward
SDT
FJC
Fourth of
July Creek
Mid-Bay
Channel
LP
Lowell
Point
Tonsina
Point
Bathtub
East
Bathtub
West
Bathtub
Thumb
Cove
Caines
Head
South
End
Sill

◀ Figure 5
Reconstructed thicknesses and initial extent of slide bodies that were mobilized during the 1964 earthquake (modified from HAEUSSLER *et al.* (2007)).

define the pre-earthquake depths in Resurrection Bay. It is assumed that the slide mass is initially at rest, and gravity is the only driving force. Although it is possible that individual slides were triggered at different times after the initial ground shaking, there is no independent evidence to support this hypothesis. Therefore we assume in the model that all slides start moving at the same time.

4.1. Movement of the Sediments and Propagation of Surface Waves

The initial thickness and extent of the slide mass is shown in Figure 5. The strong ground shaking associated with the earthquake acted as a trigger that released unstable sediments in the bay. The slide masses moved downslope, spreading out and filling the bathtub from all directions (Fig. 6). Because the bottom of the bathtub is nearly flat, slide speed decreased dramatically when the sediments reached the deepest part of the fjord (Figs. 6C, D). Only a relatively small amount of sediments from the South End slide complex (Fig. 5) moved out of the basin to the southern slope of the glacial sill that extends across the bay and keeps sediment in the basin (Fig. 6D). Results of numerical simulations show that it took about 30 minutes for the sediment flow to completely cover the bathtub.

The wave modeling results show that each slope failure produced a cylindrical wave with a crest propagating toward the opposite shore, and the trough moving toward the generation area (Fig. 7). This wave pattern is in agreement with previous numerical studies of waves generated by viscous underwater slides (THOMSON *et al.*, 2001; RABINOVICH *et al.*, 2003). In frame B ($t = 40$ sec), the wave crests from the Lowell Point (LP), Seward downtown (SDT), and Fourth of July Creek (FJC) slides are clearly visible (white dashed lines). At $t = 1$ min the crests pass the middle of the bay and continue moving toward the opposite shores, while the wave from the LP slide is approaching the southern end of Seward (Fig. 7C). At $t = 1$ min 40 sec the wave from the FJC slide hits Seward at the southeastern point of the fan delta (Frame D, white dashed line). Frames D and E show complicated patterns of multiple reflections and wave interactions in the bay. About 5 minutes after the beginning of ground shaking the wave action subsides (Fig. 7F). Our modeling results agree with the observation that sliding appeared to terminate at the end of the shaking (that lasted about 4.5 minutes), and therefore the source of the waves ceased as well. This is consistent with the assumption that most of sediments was released during the period of ground shaking.

The waves generated in the southern part of the bay by the South End and Thumb Cove slide complexes (Fig. 5) propagated mostly to the west, in the direction of Caines Head, and to the south, toward the open boundary (Figs. 7B, C). Two waves, produced by the eastern and western slides of the South End slide complex, are visible on frames C and D (yellow arrows), diffracting around Caines Head.

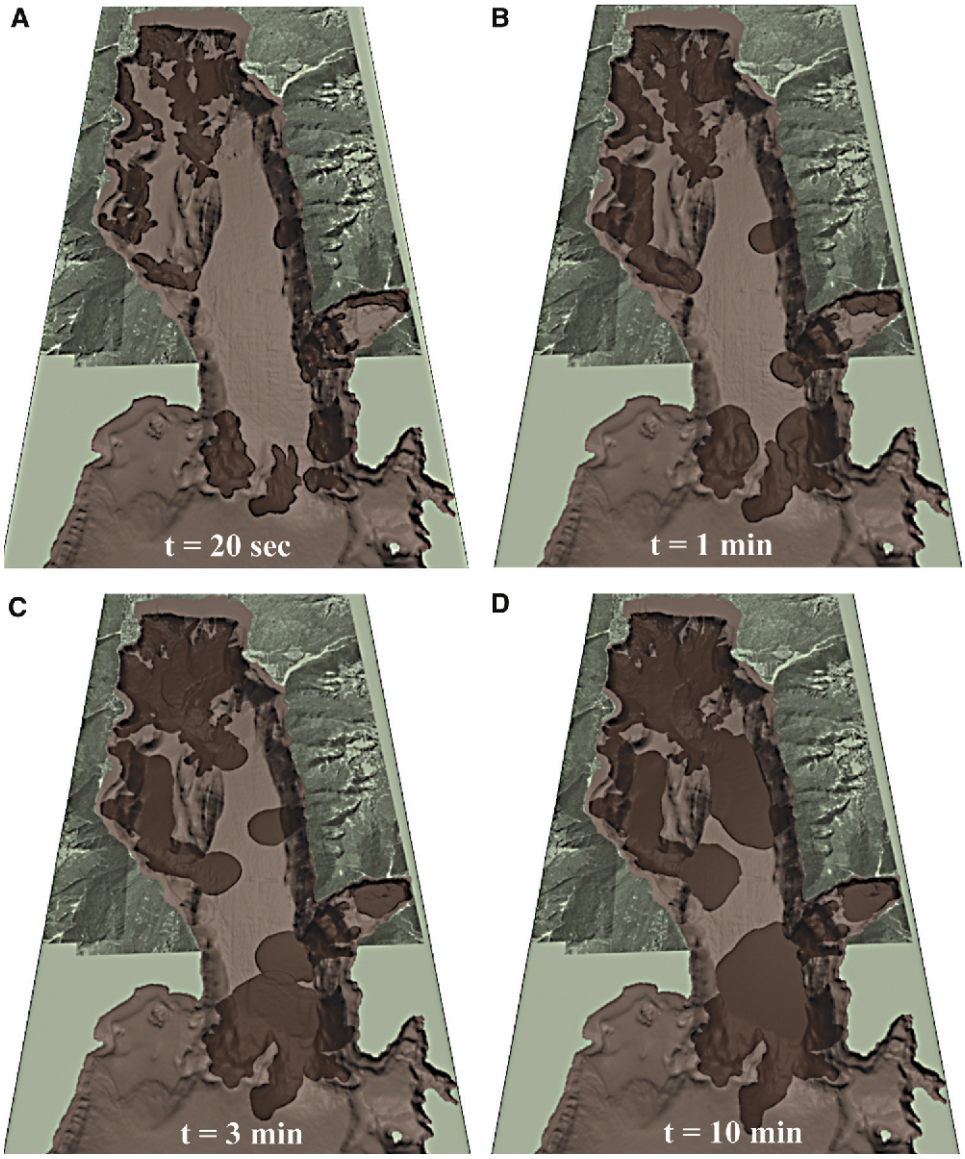

Figure 6
Snapshots from the numerical simulation of slide mass.

4.2. Simulated Wave Records

We conducted a numerical experiment to investigate how individual slide failures contributed to the observed tsunami amplitudes. The equations that describe water waves in this problem are nonlinear shallow water equations. The time series of water waves

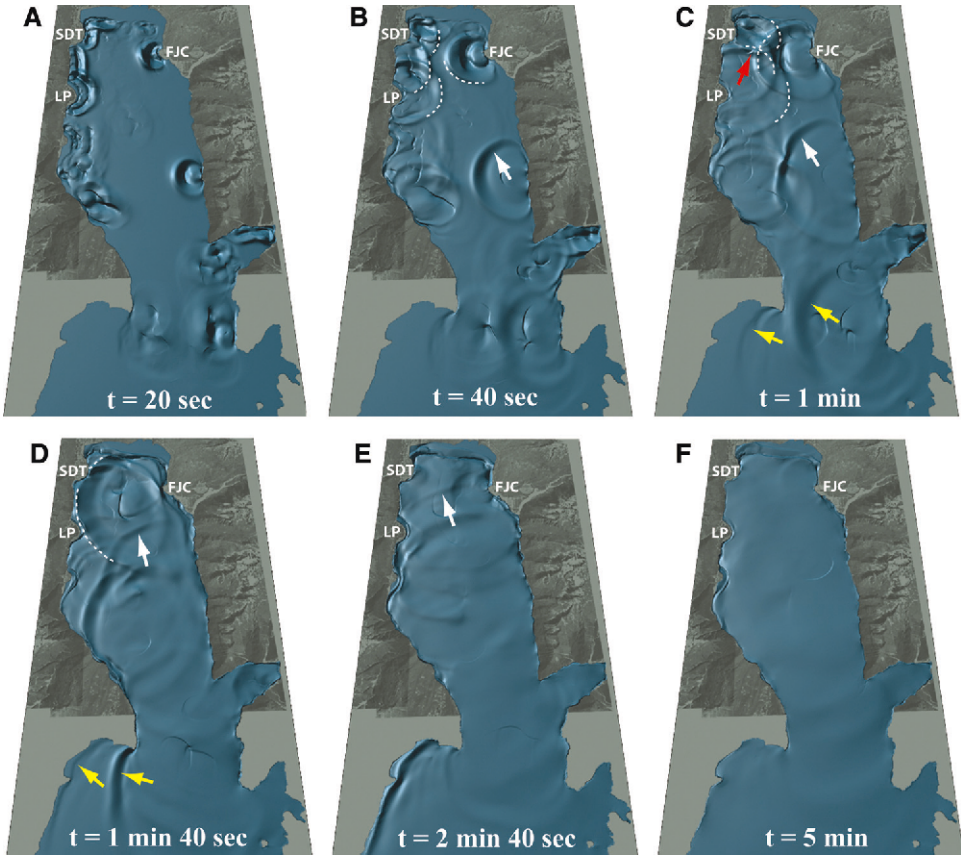

Figure 7
Snapshots from numerical simulation of surface waves in Resurrection Bay generated by the moving slide mass. Slide locations: SDT - Seward downtown, LP - Lowell Point, FJC - Fourth of July Creek. Dashed lines and arrows indicate positions of different wave fronts (see text for reference).

generated by multiple slope failures cannot generally be represented as a linear superposition of a time series of waves generated by individual slides. This is especially true if interacting waves propagate at a small angle with respect to each other and for a long enough time for nonlinear effects to grow. But in cases where the relative angles are not small, and especially when waves propagate in the opposite directions (crossing waves) with very small interaction time, the nonlinear effects can be neglected. For example, in the scope of shallow water equations, the mathematical problem of two crossing waves is equivalent to a problem of a wave reflecting from a vertical wall (PELINOVSKY, 1996), in which case the nonlinear effects have been shown to be minimal. In our analysis we superpose the waves that propagate either in the opposite directions or at angles greater than 45° with short interaction time, and therefore the linear approximation is valid.

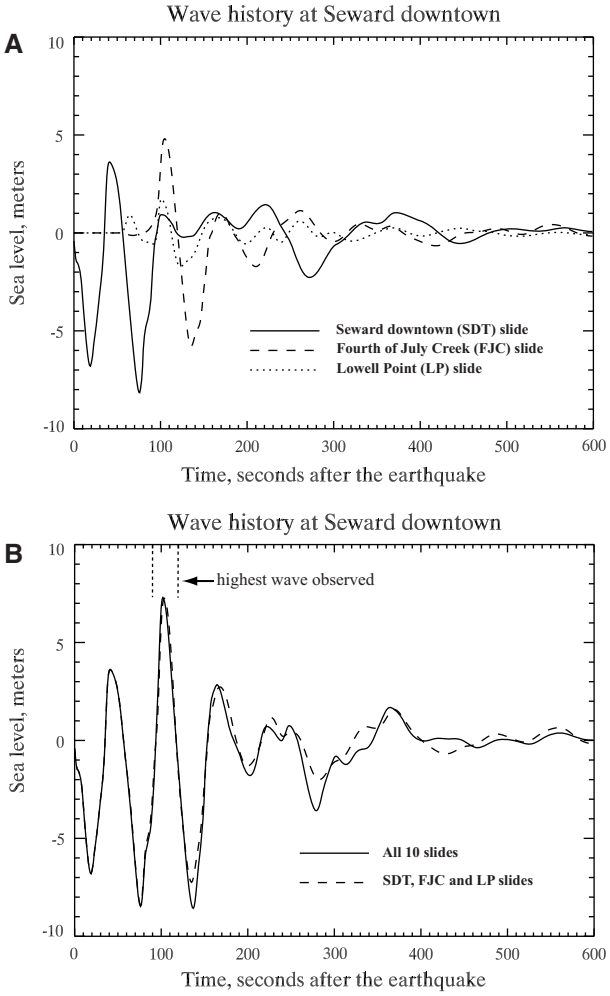

Figure 8
Simulated water level at Seward downtown.

The numerical experiment consisted of three steps. First, we selected the slides that are the closest to Seward, and also have substantial volumes and relatively shallow initiation depth. In Figure 5 these slide complexes are: SDT (Seward downtown, 27.5 million m^3), LP (Lowell Point, 18.1 million m^3) and FJC (Fourth of July Creek, 35 million m^3). We modeled each of these slides separately, and calculated time histories for generated waves at all three locations shown in Figure 2. Then, we modeled the three slides together, and calculated the time histories at the same locations. Finally, we calculated time histories for waves resulting from all 10 slides.

The results of the water level simulation at Seward are shown in Figure 8. The Seward slide first generated a trough, which was observed as a massive drawdown of

water about 30 seconds after the initial ground shaking in the waterfront area, followed by the wave crest (Fig. 8a). The highest simulated wave at Seward was the one generated by the FJC slide that arrived in 1 min 40 seconds after the earthquake. It was the superposition of this wave and two smaller crests from the Seward slide and the Lowell Point slide that resulted in the maximum observed wave height at Seward (Table 1). Figure 8b shows the time series of waves resulted from the slides SDT, LP, and FJC combined, compared to the time series of waves generated by all slides. It is evident that the waves generated by slides in the lower part of the bay had relatively little impact on the wave amplitudes in the upper bay during ground shaking (first 250 seconds).

As was the case in Seward, the initial trough at Fourth of July Creek (Fig. 9a) was generated by the local slide, but the following crest was not as high as the crest generated by the Seward slope failure. The waves from the opposite shore, induced by the SDT slide and the LP slide, arrived at Fourth of July Creek almost at the same time, in about 105 sec, and their superposition generated the highest crest at this location. This was probably the wave that, according to observations, ran inland 400 meters (WILSON and TØRUM, 1968). Figure 9b shows that the amplitude of the second trough is much smaller if the wave field is calculated from all 10 slides, compared to its amplitude produced by the slides in the upper bay only. This trough was diminished by the superimposed wave crest produced by the Bathtub East failure (Fig. 5), which arrived to Fourth of July Creek in about 140 sec. This crest is indicated by the white arrow on frames B–E of Figure 7.

The Lowell Point time series are shown in Figure 10. There is a short first positive wave at this location, due to a combination of the slide geometry and the location of the time series point (Figs. 2 and 5). The slide complex consists of two major areas, and the crest from the northern part of the slide that propagates toward the opposite shore reaches the time series point faster than the trough from the southern section of the slide complex does. The wave from Fourth of July Creek arrives at Lowell Point in 1 min 40 sec, and the wave from Seward arrives 20 sec later (Fig. 10a). Superposition of these waves (Figure 10b) generates a 6.5 m high crest at Lowell Point.

5. Discussion and Conclusions

We performed numerical simulations of tsunami waves generated by submarine slides in Resurrection Bay, Alaska, during the M_W 9.2 1964 earthquake. Our numerical results confirm the hypothesis that tsunami waves observed in Seward during and immediately after the earthquake resulted from multiple submarine slope failures (LEE *et al.*, 2006; HAEUSSLER *et al.*, 2007). Results of numerical simulation of water waves at Seward for the first 5 minutes after the initial ground shaking are in good agreement with the eyewitness observations (Fig. 8b, Table 1). Our numerical experiments were designed to investigate the relative contributions of different submarine slide complexes. The results show that the Seward downtown (SDT) slide, the Lowell Point (LP) slide, and the Fourth of July

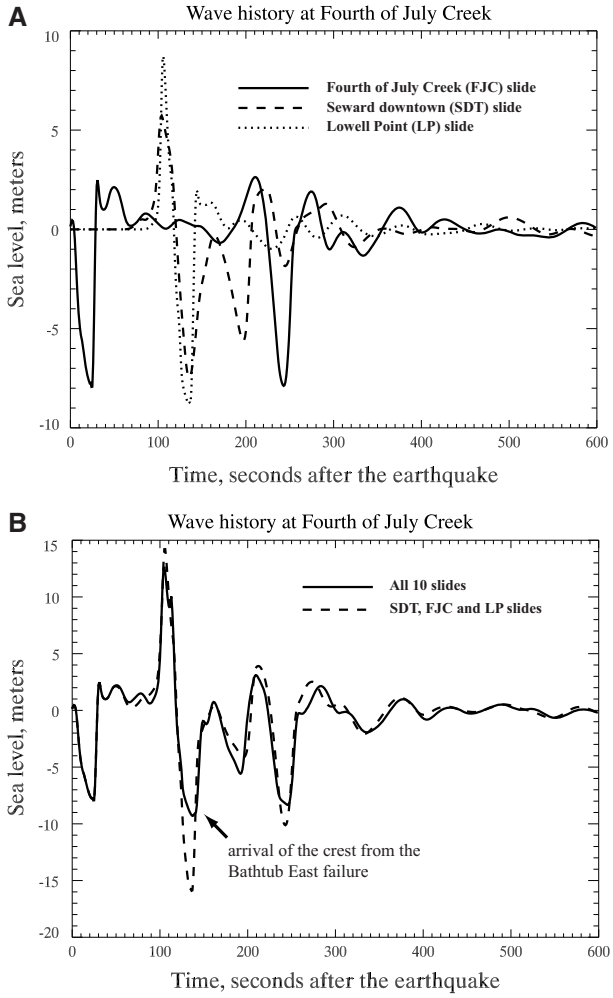

Figure 9
Simulated water level at Fourth of July Creek.

Creek (FJC) slide were the major contributors of tsunami wave energy in the upper bay during the first 3 minutes after slide initiation.

Eyewitness descriptions of events at Seward on March 27, 1964 (WILSON and TØRUM, 1968) report that a 6–8 m high, north-moving wave arrived at the Seward waterfront 1.5-2 minutes after the earthquake. The simulated time history at downtown Seward (Fig. 8b) agrees very well with observation of this wave (Table 1). Also, several observers noted the north-moving wave crossing the wave coming from the east. We interpret these observations as the interaction of the waves generated by the LP and FJC slides (Fig. 7, frame C, red arrow). The numerical results show that the highest waves at Seward were

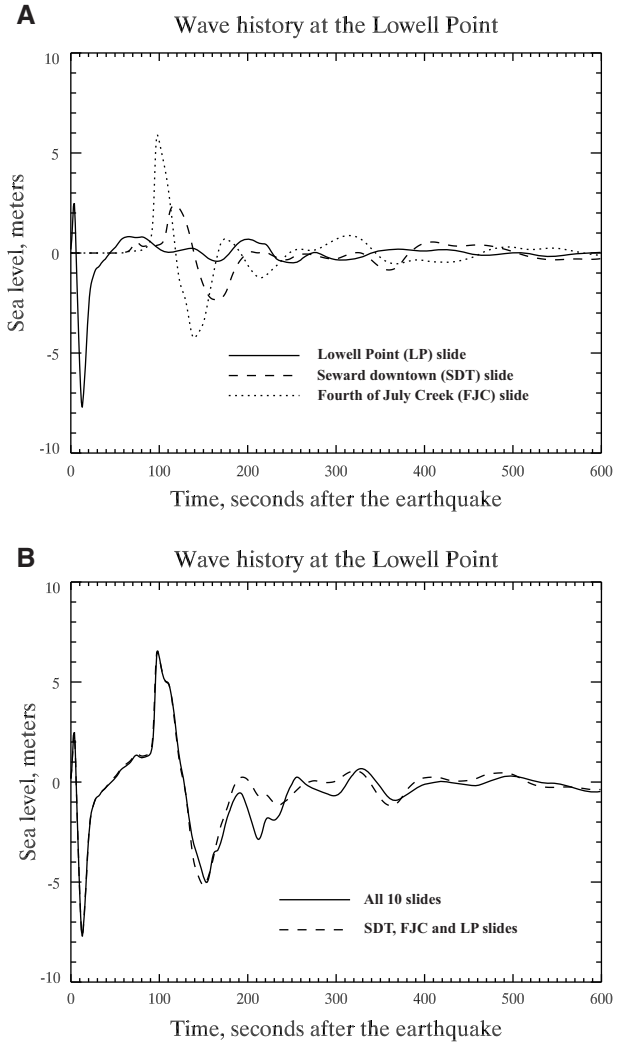

Figure 10
Simulated water level at the Lowell Point.

the result of positive interference of the three major waves in the upper part of Resurrection Bay, generated by the SDT, LP and FJC slides (Fig. 8b).

WILSON and TØRUM (1968) describe "boils" of water observed about 1.5 km west of the Fourth of July Creek and speculate they could be the result of an underwater slide. Numerical experiments conducted by FINE *et al*. (2003) show that the total wave energy generated by a slide strongly depends on the initial position of the slide. For submarine slides, wave amplitude quickly decreases when initial depth of the slide increases. It is unlikely that the sliding mass could have generated a big wave in the middle of the bay, at

a depth of about 200 m. It is possible, though, that the Mid-Bay Channel slide experienced a delayed trigger, caused by the motion of the FJC slide when the latter reached the middle of the bay and scoured the bottom (HAEUSSLER *et al.*, 2007). This would have caused a significant increase in the total volume of the moving mass. This hypothesis could be verified by additional numerical experiments.

Observers at Lowell Point reported a wave coming from Seward, and at the same time, a wave radiating toward Fourth of July Creek (WILSON and TØRUM, 1968). We interpret these observations as waves generated by SDT and LP slides. The highest reported wave at Lowell Point was about 6 m high (WILSON and TØRUM, 1968), which agrees with the modeling results (Fig. 10b).

Future work will include simulation of runup of tsunami waves generated by slope failures in Resurrection Bay and comparison of results with inundation patterns observed in 1964. For the purposes of tsunami hazard mitigation, we plan to study tsunami waves generated by hypothetical underwater slides and estimate the landslide tsunami hazard. Engineering studies conducted after the 1964 earthquake in Seward and Valdez (LEMKE, 1967; COULTER and MIGLIACCIO, 1966; SHANNON and HILTS, 1973) concluded that underwater slope failures have not improved slope stability, meaning that the same slopes could fail again during the next large earthquake. Moreover, some of the streams draining into Resurrection Bay, such as Lowell Creek and Fourth of July Creek, have been rerouted by humans. These creeks are now depositing sediments in new locations, which may lead to new unstable sediment accumulations and future submarine slides.

Acknowledgments

This study was supported by NOAA grants 27-014d and 06-028a through Cooperative Institute for Arctic Research, and by the USGS. We thank Michelle Coombs, Chris Waythomas and anonymous reviewers for helpful suggestions that improved this manuscript. The authors also thank Keith Labay for the construction of the high-resolution DEM of Resurrection Bay, and Dave West for data processing in ArcGIS and his help in preparing the figures. Numerical calculations for this work are supported by a grant of High Performance Computing (HPC) resources from the Arctic Region Supercomputing Center (ARSC) at the University of Alaska Fairbanks as part of the US Department of Defense HPC Modernization Program. We thank ARSC specialists Miho Aoki and Sergei Maurits for visualizations of computational results.

REFERENCES

ASSIER-RZADKIEWICZ, S., MARIOTTI, C., and HEINRICH, P. (1997), *Numerical simulation of submarine landslides and their hydraulic effects*, J. Waterw. Port. Coast. Ocean. Eng. *123*(4), 149–157.

BERG, E., COX, D., FURUMOTO, A., KAJIURA, K., KAWASUMI, H., and SHIMA, E. (1964), *Field survey of the tsunami of 28 March 1964 in Alaska*, Report, Hawaii Institute of Geophysics (unpublished).

BORNHOLD, B., THOMSON, R., RABINOVICH, A., KULIKOV, E., and FINE, I. (2001), *Risk of landslide-generated tsunamis for the coast of British Columbia and Alaska*. In *An Earth Odyssey*, Proc. Canadian Geotechn. Conf., pp. 1450–1454.

COULTER, H. and MIGLIACCIO, R. (1966), *Effects of the Earthquake of March 27, 1964, at Valdez, Alaska*, U.S. Geolog. Survey Prof. Paper 542-C, 36 pp.

FINE, I., RABINOVICH, A., KULIKOV, E., THOMSON, R., and BORNHOLD, B. (1998), *Numerical modelling of landslide-generated tsunamis with application to the Skagway Harbor tsunami of November 3, 1994*. In Proc. Int. Conf. on Tsunamis, Paris, pp. 211–223.

FINE, I., RABINOVICH, A., THOMSON, R., and KULIKOV, E., *Numerical modeling of tsunami generation by submarine and subaerial landslides*. In: *Submarine Landslides and Tsunamis*, (Yalciner, A., Pelinovsky, E., Okal, E., Synolakis, C., eds.), (Kluwer 2003), pp. 69–88.

GRILLI, S. and WATTS, P. (2005), *Tsunami generation by submarine mass failure. I : Modeling, experimental validation, and sensitivity analysis*, J. Waterw. Port. Coast. Ocean. Eng. *131*(6), 283–297, DOI 10.1061/(ASCE)0733-950X(2005)131:6(283).

HAEUSSLER, P., LEE, H., RYAN, H., LABAY, K., KAYEN, R., HAMPTON, M., and SULEIMANI, E. (2007), *Submarine slope failures near Seward, Alaska, during the M9.2 1964 earthquake*. In: *Submarine Mass Movements and their Consequences*, (Lykousis, V., Sakellariou, D., Locat, J., eds.), pp. 269–278.

HAMPTON, M., LEE, H., and LOCAT, J. (1996), *Submarine landslides*, Rev. Geophys. *34*, 33–59.

HAMPTON, M., LEMKE, R., and COULTER, H. (2002), *Submarine landslides that had a significant impact on man and his activities: Seward and Valdez, Alaska*. In: *Submarine Landslides: Selected Studies in the US Exclusive Economic Zone*, (Schwab, W., Lee, H., Twichell, D., eds.), U.S. Geolog. Survey Bull., pp. 123–134.

HARBITZ, C. (1992), *Model simulations of tsunamis generated by the Storegga Slides*, Marine Geol. *105*, 1–21.

IMAMURA, F., HASHI, K., and IMTEAZ, M., *Modeling for tsunamis generated by landsliding and debris flow*. In: *Tsunami Research at the End of a Critical Decade*, (Hebenstreit, G.T., ed.), (Kluwer 2001), pp. 209–228.

JIANG, L. and LEBLOND, P. (1992), *The coupling of a submarine slide and the surface waves which it generates*, J. Geophys. Res. *97*(C8), 12,731–12,744.

JIANG, L. and LEBLOND, P. (1994), *Three-dimensional modeling of tsunami generation due to a submarine mudslide*, J. Phys. Oceanogr. *24*(3), 559–572.

KULIKOV, E., RABINOVICH, A., FINE, I., BORNHOLD, B., and THOMSON, R. (1998), *Tsunami generation by landslides at the Pacific coast of North America and the role of tides*, Oceanology *38*(3), 361–367.

LABAY, K. and HAEUSSLER, P. (2008, in press), *Combined high-resolution LIDAR topography and multibeam bathymetry for upper Resurrection Bay, Seward, Alaska*, U.S. Geolog. Survey Digital Data Series.

LANDER, J. (1996), *Tsunamis affecting Alaska. 1737–1996*, No. 31 in NGDC Key to Geophysical Research, National Geophysical Data Center, Boulder, Colorado.

LANTZ, B. and KIRKPATRICK, M., *Seward Quake, Good Friday, 1964* (Kirkpatrick Printing Co., Seward, Alaska 1964).

LEE, H., SCHWAB, W., and BOOTH, J. (2002), *Submarine landslides: An introduction*. In: *Submarine Landslides: Selected Studies in the U.S. Exclusive Economic Zone*, (Schwab, W., Lee, H., Twichell, D., eds.), U.S. Geolog. Survey Bull., pp. 1–13.

LEE, H., RYAN, H., KAYEN, R., HAEUSSLER, P., DARTNELL, P., and HAMPTON, M. (2006), *Varieties of submarine failure morphologies of seismically-induced landslides in Alaska fjords*, Norwegian J. Geology *86*, 221–230.

LEMKE, R. (1967), *Effects of the Earthquake of March 27, 1964, at Seward, Alaska*, U.S. Geolog. Survey Prof. Paper 542-E, 48 pp.

LYNETT, P. and LIU, P.F. (2002), *A numerical study of submarine landslide generated waves and runup*, Proc. Roy. Soc. London *A 458*, 2885–2910.

LYNETT, P. and LIU, P.F. (2004a), *A two-layer approach to water wave modeling*, Proc. Roy. Soc. London *A 460*, 2637–2669.

LYNETT, P. and LIU, P.F. (2004b), *Linear analysis of the multi-layer model*, Coastal Eng. *51*, 439–454.

LYNETT, P. and LIU, P.F. (2005), *A numerical study of the runup generated by three-dimensional landslides*. J. Geophys. Res. *110*(C03006), DOI 10.1029/2004JC002443.

PELINOVSKY, E. (1996), *Tsunami Waves Hydrodynamics*, Institute of Appl. Phys., RAS, Nizhny Novgorod, Russia.

PLAFKER, G., KACHADOORIAN, R., ECKEL, E., and MAYO, L. (1969), *Effects of the Earthquake of March 27, 1964 on various communities*, U.S. Geolog. Survey Prof. Paper *542-G*, 50 pp.

RABINOVICH, A.B., THOMSON, R.E., BORNHOLD, B.D., FINE, I.V., and KULIKOV, E.A. (2003), *Numerical modelling of tsunamis generated by hypothetical landslides in the Strait of Georgia, British Columbia*, Pure Appl. Geophys. *160*(7), 1273–1313.

SAVOIE, M., SAVOIE, J., TREFRY, J., SEMMLER, C., WOODALL, D., TROCINE, R., BROOKS, J., and MCDONALD, T. (2006), *Port Valdez sediment coring program: Final 2004 monitoring report*, Kinnetic Laboratories, Inc., Contract No. 961.04.1 for Prince William Sound Regional Citizens' Advisory Council.

SHANNON, W. and HILTS, D., *Submarine landslide at Seward*. In *The Great Alaska Earthquake of 1964*. Engin. (National Academy of Sciences Washington, D.C. 1973), pp. 144–156.

THOMSON, R.E., RABINOVICH, A.B., KULIKOV, E.A., FINE, I.V., and BORNHOLD, B.D., *On numerical simulation of the landslide-generated tsunami of November 3, 1994 in Skagway Harbor, Alaska*. In: *Tsunami Research at the End of a Critical Decade* (Hebenstreit, G.T., ed.), (Kluwer 2001), pp. 243–282.

TITOV, V. and GONZALEZ, F., *Numerical study of the source of the July 17, 1998 PNG tsunami*. In: *Tsunami Research at the End of a Critical Decade*, (Hebenstreit, G.T., ed.), (Kluwer 2001), pp. 197–207.

WILSON, B. and TØRUM, A. (1968), *The tsunami of the Alaskan Earthquake, 1964: Engineering evaluation*, U.S. Army Corps of Engineers, Technical Memo. *25*, 401 pp.

(Received February 16, 2008, accepted June 18, 2008)
Published Online First: February 6, 2009